Large Third-Order Electronic Polarizability of a Conjugated Porphyrin Polymer

Stephen M. Kuebler,[†,§] Robert G. Denning,*[,†] and Harry L. Anderson[‡]

Contribution from the Inorganic Chemistry Laboratory, University of Oxford, South Parks Road, Oxford, U.K., OX1 3QR, and the Dyson Perrins Laboratory, University of Oxford, South Parks Road, Oxford, U.K., OX1 3QY

Received June 28, 1999

Abstract: Degenerate four-wave mixing measurements, using 45 ps pulses at 1064 nm, have been used to determine the magnitude of the third-order optical susceptibility tensor for thin films of a conjugated porphyrin polymer. The time dependence of the signals indicates that the dominant response is fast relative to the duration of the optical pulses. It is shown that a response on this time scale cannot be consistent with a mechanism in which resonant absorption is significant, and therefore that the primary component of the susceptibility must correspond to an instantaneous electronic polarization. The microscopic polarizability per macrocycle of the polymer is approximately 3 orders of magnitude greater than that of the monomer—a result that indicates the role of inter-macrocycle conjugation in the nonlinearity. This appears to be the largest one-photon−off-resonance third-order optical susceptibility reported for any organic material.

Introduction

The realization of a practical all-optical switch has been frustrated by the absence of materials that combine suitably large optical nonlinearities with adequate transparency. The response time of the nonlinearity is also vital, if ultrafast switching times are to be achieved, and ideally this should be short compared with the period of an optical cycle. Conjugated organic polymers, such as polydiacetylenes, come closest to meeting these requirements, although currently they do not offer large enough nonlinearities together with suitably fast response times.[1]

In the search for improved materials, the structural and electronic properties of porphyrins are attractive. In particular they have strong electronic transitions ($\varepsilon_{max} \approx 10^4-10^5$ M^{-1} cm^{-1}) in the visible and near infrared (NIR), whose energies can be shifted, both by chemically modifying the ring and by changing the coordinated metal. Because these transitions are unusually sharp (fwhm $\approx$ 500−1500 cm^{-1}),[2] the nonlinear susceptibilities may be enhanced near-resonance, without incurring significant linear absorption losses. Porphyrins and phthalocyanines are chemically and thermally robust, surviving to over 400 °C in some cases,[2] and are stable under intense optical irradiation.[3]

The optical nonlinearities of some of these species have been investigated. For example, metalloporphyrins and metallophthalocyanines are promising for optical limiting,[4,5] and their potential for all-optical switching has also been actively explored.[6−16] A silicon naphthalocyanine has been used as a saturable absorber in a nonlinear Fabry−Perot etalon to demonstrate optical bistability.[17] These results, together with the large susceptibilities of polydiacetylenes, suggest that conjugated porphyrin polymers may be promising nonlinear optical (NLO) materials.

The conjugated porphyrin polymer **1** consists of zinc-containing porphyrin units, edge-linked at the *meso*-position by butadiyne fragments. The synthesis and characterization of this polymer has been reported previously.[18] Small-angle neutron scattering indicates that the average degree of polymerization,

* To whom correspondence should be addressed.
† Inorganic Chemistry Laboratory.
‡ Dyson Perrins Laboratory.
§ Current address: Department of Chemistry, The University of Arizona, 1306 E. University Blvd., Tucson, AZ 85721.

(1) Stegeman, G.; Likamwa, P. In *Nonlinear Optical Materials and Devices for Applications in Information Technology*; Miller, A., Welford, K. R. and Daino, B., Eds.; Vol. 289; Kluwer Acad. Publ.: Dordrecht, 1995; pp 285−320.
(2) Gouterman, M. In *The Porphyrins*; Dolphin, D., Ed.; Vol. 3; Academic: New York, 1978; pp 1−165.
(3) Berezin, B. D. *Coordination Compounds of Porphyrins and Phthalocyanines*; Wiley: New York, 1981.
(4) Perry, J. W.; Mansour, K.; Marder, S. R.; Perry, K. J.; Alvarez, D., Jr.; Choong, I. *Opt. Lett.* **1994**, *19*, 625−627.
(5) McEwan, K. J.; Robertson, J. M.; Anderson, H. L.; Wylie, A. P. *Mater. Res. Soc. Symp. Proc.* **1997**, *479*, 29−39.
(6) Ho, Z. Z.; Ju, C. Y.; Hetherington, W. M., III. *J. Appl. Phys.* **1987**, *62*, 716−718.
(7) Maloney, C.; Byrne, H.; Dennis, W. M.; Blau, W. *Chem. Phys.* **1988**, *121*, 21−39.
(8) Kaltbeitzel, A.; Neher, D.; Bubeck, C.; Sauer, T.; Wegner, G.; Caseri, W. In *Electronic Properties of Conjugated Polymers III*; Kuzmany, H., Mehring, M. Roth, S., Eds.; Springer Series in Solid-State Sciences; Springer: Berlin, 1989; Vol. 91, pp 220−224.
(9) Casstevens, M. K.; Samoc, M.; Pfleger, J.; Prasad, P. N. *J. Chem. Phys.* **1990**, *92*, 2019−2024.
(10) Wang, N. Q.; Cai, Y. M.; Heflin, J. R.; Garito, A. F. *Mol. Cryst. Liq. Cryst.* **1990**, *189*, 39−48.
(11) Wang, N. Q.; Cai, Y. M.; Heflin, J. R.; Wu, J. W.; Rodenberger, D. C.; Garito, A. F. *Polymer* **1991**, *32*, 1752−1755.
(12) Grund, A.; Kaltbeitzel, A.; Mathy, A.; Schwarz, R.; Bubeck, C.; Vermehren, P.; Hanack, M. *J. Phys. Chem.* **1992**, *96*, 7450−7454.
(13) Norwood, R. A.; Sounik, J. R. *Appl. Phys. Lett.* **1992**, *60*, 295−297.
(14) Guha, S.; Kang, K.; Porter, P.; Roach, J. R.; Remy, D. E.; Aranda, F. J.; Rao, D. V. G. L. N. *Opt. Lett.* **1992**, *17*, 264−266.
(15) Reeves, R. J.; Powell, R. C.; Ford, W. T.; Chang, Y. H.; Zhu, W. In *Electrical, Optical, and Magnetic Properties of Organic Solid State Materials*; Chiang, L. Y., Garito, A. F., Sandman, D. J., Eds.; Materials Research Society Symposium Proceedings; Material Research Society: Pittsburgh, 1992; Vol. 247, pp 203−208.
(16) Suslick, K. S.; Chen, C.-T.; Meredith, G. R.; Cheng, L.-T. *J. Am. Chem. Soc.* **1992**, *114*, 6928−6930.
(17) Garito, A. F.; Wu, J. W. *Proc. Soc. Photo-Opt. Instrum. Eng.* **1989**, *1147*, 2−11.
(18) Anderson, H. L.; Martin, S. J.; Bradley, D. D. C. *Angew. Chem., Int. Ed. Engl.* **1994**, *33*, 655−657.

10.1021/ja9922330 CCC: $19.00
Published on Web 12/31/1999

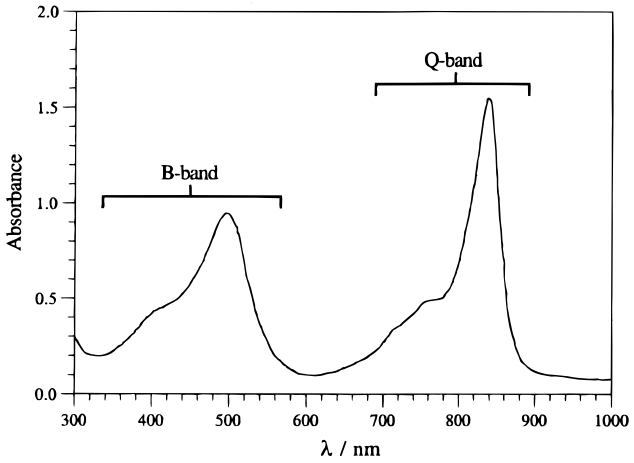

Figure 1. Absorption spectrum of a 160-nm thick film of the porphyrin polymer **1**. The absorbance has not been corrected for losses due to reflection.

n, is ∼10−15. Attempts to detect the end-groups by ^{1}H NMR and FT IR spectroscopy have been unsuccessful, but they are probably terminal alkynes. This polymer is extremely soluble in chlorinated solvents, in the presence of ligands such as pyridine, due to the large aliphatic *R*-groups on the macrocycle.

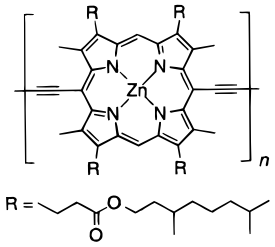

Polymer **1**

Many spectroscopic measurements have been performed on this material, including optical absorption,[18,19] quadratic electroabsorption (QEA, Stark spectroscopy),[18,20] polarized electronic absorption,[21] field-induced absorption,[22] femtosecond transient absorption,[19,23] field-dependent transient absorption,[24] time-resolved microwave conductivity,[25] and optical limiting.[26] The solid-state electronic absorption spectrum of a thin film of polymer **1** (Figure 1) consists of two bands at 500 and 860 nm. The spectrum is very similar to that of the polymer in solution, although the band at 860 nm is significantly sharper in the solid-state. Comparison of this spectrum with those of a series of monomeric to hexameric model oligomers[18,27] shows that these bands are derived from the *B*- and *Q*-bands of the porphyrin monomer. The *Q*-band of the polymer is significantly red-shifted and intensified, compared with the *Q*-band of the simple porphyrin, which indicates that there is substantial delocalization across the butadiyne bridges.[18,19] Consistent with this interpretation, the Stark effect observed in QEA experiments increases with the chain length,[18] while time-resolved microwave conductivity experiments demonstrate high charge mobility within polymer chains.[25] This contrasts with the situation in most previously studied porphyrin oligomers and polymers which are not conjugated and exhibit only weak exciton coupling interactions between neighboring porphyrin units.[12,28−33] Several alkyne-linked[34−39] and edge-fused[40−43] conjugated dimers and trimers have been investigated,[44] but there is still only one other report of a soluble conjugated porphyrin polymer.[45] *meso*-Alkynyl porphyrins with donor−acceptor groups exhibit delocalization similar to that of polymer **1**, resulting in strong second-order NLO behavior.[46,47]

Compared to the classic conjugated polymers such as polyacetylene and polydiacetylene (PDA), which have absorption edges in the visible,[48] the sharpness and high intensity of the NIR *Q*-band of the porphyrin polymer should offer a stronger one-photon resonant enhancement of the third-order susceptibility in the telecommunications windows near 1.3 and 1.5 μm, together with good transparency.[20] The nonlinearity in the region of the *Q*-band has been examined by QEA spectroscopy,[18,20] and *Z*-scan measurements have been made at 532 nm.[26] However, the quantity of most direct relevance for all-optical switching near 1.5 μm is the third-order susceptibility tensor $\tilde{\chi}^{(3)}(-\omega;\omega,\omega,-\omega)$ for the case where ω lies in the transparent region to the red side of the *Q*-band. In this paper we report the use of degenerate four-wave mixing (DFWM) at 1064 nm to measure the principal components of this tensor and show that its magnitude compares well with the susceptibilities of existing materials.

(19) Beljonne, D.; O'Keefe, G. E.; Hamer, P. J.; Friend, R. H.; Anderson, H. L.; Brédas, J. L. *J. Chem. Phys.* **1997**, *106*, 9439−9460.
(20) Martin, S. J.; Anderson, H. L.; Bradley, D. D. C. *Adv. Mater. Opt. Electron.* **1994**, *4*, 277−283.
(21) Anderson, H. L. *Adv. Mater.* **1994**, *6*, 834−836.
(22) Pichler, K.; Anderson, H. L.; Bradley, D. D. C.; Friend, R. H.; Hamer, P. J.; Harrison, M. G.; Jarrett, C. P.; Martin, S. J.; Stephens, J. A. *Mol. Cryst. Liq. Cryst.* **1994**, *256*, 415−422.
(23) O'Keefe, G. E.; Denton, G. J.; Harvey, E. J.; Phillips, R. T.; Friend, R. H.; Anderson, H. L. *J. Chem. Phys.* **1996**, *104*, 805−811.
(24) O'Keefe, G. E.; Halls, J. J. M.; Walsh, C. A.; Denton, G. J.; Friend, R. H.; Anderson, H. L. *Chem. Phys. Lett.* **1997**, *276*, 78−83.
(25) Piet, J. J.; Warman, J. M.; Anderson, H. L. *Chem. Phys. Lett.* **1997**, *266*, 70−74.
(26) Qureshi, F. M.; Martin, S. J.; Long, X.; Bradley, D. D. C.; Henari, F. Z.; Blau, W. J.; Smith, E. C.; Wang, C. H.; Kar, A. K.; Anderson, H. L. *Chem. Phys.* **1998**, *231*, 87−94.
(27) Anderson, H. L. *Inorg. Chem.* **1994**, *33*, 972−981.
(28) Wasielewski, M. R. *Chem. Rev.* **1992**, *92*, 435−461.
(29) Bao, Z. N.; Yu, L. P. *Trends Polym. Sci.* **1995**, *3*, 159−164.
(30) Sauer, T.; Caseri, W.; Wegner, G. *Mol. Cryst. Liq. Cryst.* **1990**, *183*, 387−402.
(31) Bao, Z. N.; Chen, Y. M.; Yu, L. P. *Macromolecules* **1994**, *27*, 4629−4631.
(32) Terazima, M.; Hitoshi, S.; Osuka, A. *J. Appl. Phys.* **1997**, *81*, 2946−2951.
(33) Sinha, A. K.; Bihari, B.; Mandal, B. K.; Chen, L. *Macromolecules* **1995**, *28*, 5681−5683.
(34) Arnold, D. P.; Heath, G. A.; James, D. A. *New J. Chem.* **1998**, 1377−1387.
(35) Arnold, D. P.; James, D. A. *J. Org. Chem.* **1997**, 3460−3469.
(36) Kumble, R.; Palese, S.; Lin, V. S.-Y.; Therien, M. J.; Hochstrasser, R. M. *J. Am. Chem. Soc.* **1998**, *120*, 11489−11498.
(37) LeCours, S. M.; DiMagno, S. G.; Therien, M. J. *J. Am. Chem. Soc.* **1996**, *118*, 11854−11864.
(38) Lin, V. S.-Y.; DiMagno, S. G.; Therien, M. J. *Science* **1994**, *264*, 1105−1111.
(39) Angiolillo, P. J.; Lin, V. S.-Y.; Vanderkooi, J. M.; Therien, M. J. *J. Am. Chem. Soc.* **1995**, *117*, 12514−12527.
(40) Reimers, J. R.; Lu, T. X.; Crossley, M. J.; Hush, N. S. *Chem. Phys. Lett.* **1996**, *256*, 353−359.
(41) Jaquinod, L.; Senge, M. O.; Pandey, R. K.; Forsyth, T. P.; Smith, K. M. *Angew. Chem., Int. Ed. Engl.* **1996**, *35*, 1840−1842.
(42) Jaquinod, L.; Siri, O.; Khoury, R. G.; Smith, K. M. *Chem. Commun.* **1998**, 1261−1262.
(43) Johnson, C. K.; Dolphin, D. *Tetrahedron Lett.* **1998**, *39*, 4753−4756.
(44) Anderson, H. L. *Chem. Commun.* **1999**, 2323−2330.
(45) Jiang, B.; Yang, S.-W.; Barbini, D. C.; Jones, W. E., Jr. *Chem. Commun.* **1998**, 213−214.
(46) Karki, L.; Vance, F. W.; Hupp, J. T.; LeCours, S. M.; Therien, M. J. *J. Am. Chem. Soc.* **1998**, *120*, 2606−2611.
(47) Yeung, M.; Ng, A. C. H.; Drew, M. G. B.; Vorpagel, E.; Brietung, E. M.; McMahon, R. J.; Ng, D. K. P. *J. Org. Chem.* **1998**, *63*, 7143−7150.
(48) Brédas, J.-L.; Silbey, R., Eds.; *Conjugated Polymers: The Novel Science and Technology of Highly Conducting and Nonlinear Optically Active Materials*; Kluwer Academic Publishers: Dordrecht, 1991.

Experimental Section

Preparation and Physical Characteristics of the Porphyrin Polymer Films. Polymer **1** was synthesized as described by Anderson *et al.*[18] Neat thin films were prepared by spin-coating a solution of the polymer in 1% pyridine/CH_2Cl_2 onto glass substrates. The pyridine promotes the dissolution of the polymer. Elemental analysis of the dry films was consistent with that expected for the pure polymer, implying that no pyridine is occluded. No birefringence was detectable between crossed polarizers, and the X-ray diffraction patterns were featureless, indicating that the films were both glassy and isotropic. The DFWM measurements were made on two films, for which the thicknesses were determined to be 160 ± 30 nm and 650 ± 100 nm, using a combination of scanning optical microscopy (SOM, Laser Tec, model 1LM11, $\lambda =$ 632.8 nm), atomic force microscopy (AFM, Park Scientific Instruments), and linear absorption measurements at 740 nm. The uncertainty in both values is due to the variation in the thickness across the sample.

Films of the polymer are bleached when exposed to air and room light for long periods (30 days), but no deterioration is observed over a period of at least six months when the materials are stored in the dark. Mechanically the films are quite fragile; they are waxy and can be rubbed off easily. However, they can be easily handled in air and room light within the time required for DFWM measurements.

Laser Characteristics. The laser used is an extensively modified, flashlamp-pumped, passively *Q*-switched and mode-locked Nd:YAG unit (based on a Spectron Laser Systems model MCB-1) with a 1.8 m linear cavity, operating at 1064 nm in the TEM_{00} mode. The round-trip time of 12.16 ns facilitates single-pulse selection. Hybrid passive/active mode-locking is achieved with an intra-cavity acousto-optic modulator (Gooch and Housego, model ML 41−4G) that is resonant at 41.131 MHz at 31.8 °C. The rf supply is gated to minimize power dissipation. The passive *Q*-switching and mode-locking dyes are either A9740 or A9860 (Kodak *Q*-switch I or II).

The most intense pulse is selected from the center of the mode-locked train of ~8 pulses using a transverse KDP electrooptic modulator (LeySop EM 200K). The modulator is driven by a Kentech Pulse-Picker/Pulse-Generator (PPPG), triggered by a fast photodiode that monitors a partial reflection from within the laser cavity. Noncollinear SHG intensity-correlation experiments indicate that the pulses are nearly transform-limited, with an average single-pulse width (fwhm) of $\tau_p =$ 45 ± 5 ps. A typical pulse has an energy of ~1 mJ with shot-to-shot fluctuations of ±20%. The output energy can be continuously attenuated using a rotating half-wave plate under computer control.

DFWM Configurations. Figures 2 and 3 show schematically the two beam-configurations used in the DFWM experiments. In the first configuration, the forward- and backward-pump beams (F-pump and B-pump) nearly counter-propagate (NCP) as they impinge on the sample, the angle between them in the vertical plane being $\theta_B = 1.6°$. A third beam, the Probe, is also incident on the sample at an angle to the F-pump in the horizontal plane of $\theta_P = 1.6°$. The angular separation between the F-pump and the B-pump causes the Signal beam to propagate in a direction that is spatially distinct from the Probe. In this respect, NCP-DFWM provides an advantage over the more traditional phase-conjugate geometry (PC-DFWM).[49] In PC-DFWM, the F-pump and B-pump strictly counter-propagate, which causes the Signal beam to travel antiparallel to the Probe. Some signal strength is inevitably sacrificed since a beam-splitter must be inserted into the path of the Probe and the Signal to isolate the Signal for detection. In contrast, the Signal and the Probe are spatially separated in NCP-DFWM, so that the entire Signal is available for detection. It can be shown that the slightly imperfect phase-matching of the signal wave in NCP-DFWM has a negligible effect on its intensity.[50] We refer to the second configuration as the forward scattering (FS) geometry. Elsewhere it has been called the "folded-box" geometry.[51−53] For both NCP- and FS-DFWM, optical delays (τ_d) of up to 2630 and 3300 ps could be introduced into two of the three incident beams, permitting complete control of the incident pulse sequence.

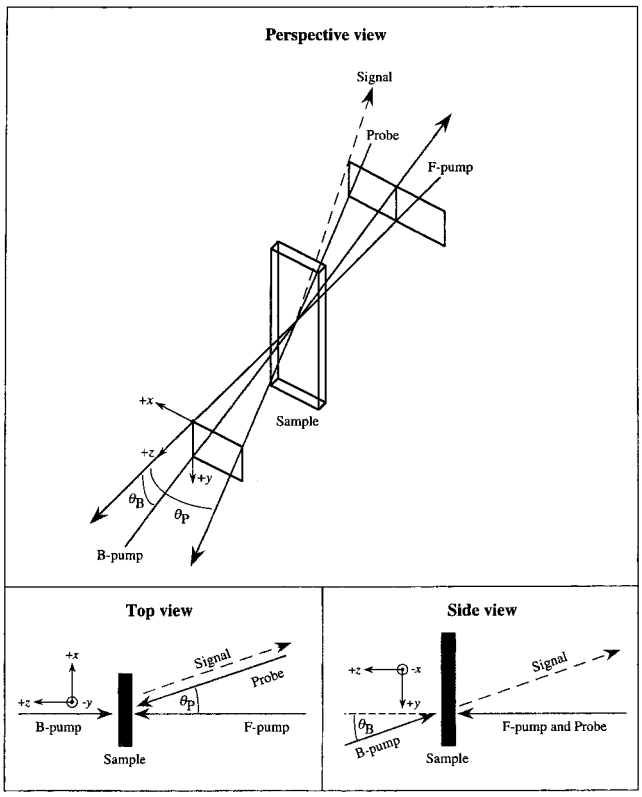

Figure 2. Schematic of the NCP-DFWM configuration showing the incident beams (F-pump, B-pump, and Probe) and the Signal beam produced by the DFWM interaction. Views of the experiment as seen along the *y*-axis (top-view) and *x*-axis (side-view) are included below the perspective drawing. The angles between the incident beams are $\theta_P = 1.6°$ and $\theta_B = 1.6°$.

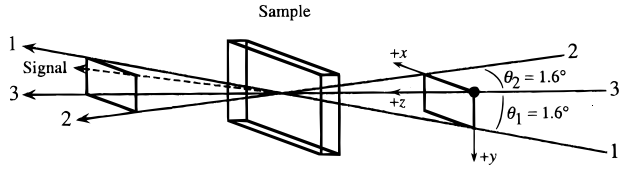

Figure 3. Schematic of the FS-DFWM configuration. The nonlinear interaction of the incident beams 1, 2, and 3 produces the Signal beam.

The main difference between the two configurations is the presence in the NCP experiment of an optically induced grating with a *fine* spatial period of $\Lambda = 0.35$ μm, formed by the interference of the Probe and the B-pump, in addition to a *coarse* grating ($\Lambda = 38$ μm) due to the Probe and the F-pump. In FS-DFWM both gratings have a coarse period, beam 3 being instrumental in the formation of both of them.[54] The principle advantage of the FS geometry is that the acoustic transit time across a coarse grating period is very large compared to the pulse duration, so that acoustic effects do not contribute to the signal.[55] However, this is not true of the fine grating in the NCP experiment.

The optical layouts include linear polarizers in all four beams paths, enabling the measurement of all of the relevant tensor components of the susceptibility $\chi^{(3)}_{ijkl}$. The notation for the NCP configuration associates the *i*, *j*, *k*, and *l* polarized fields of the tensor with the Signal, F-pump, B-pump, and Probe beams respectively, while in the FS

(49) Caro, R. G.; Gower, M. C. *IEEE J. Quantum Electron.* **1982**, *18*, 1376−1380.

(50) Kuebler, S. M. Studies of the third-order nonlinear optical properties of some materials by degenerate four-wave mixing. D. Phil. Thesis, University of Oxford, 1997.

(51) Shirley, J. A.; Hall, R. J.; Eckbreth, A. C. *Opt. Lett.* **1980**, *5*, 380−382.

(52) Beddard, G. S.; McFadyen, G. G.; Reid, G. D.; Thorne, J. R. G. *Chem. Phys.* **1993**, *172*, 363−376.

(53) Carter, G. M. *J. Opt. Soc. Am. B* **1987**, *4*, 1018−1024.

(54) Eichler, H. J.; Günter, P.; Pohl, D. W. *Laser-Induced Dynamic Gratings*, Springer Series in Optical Sciences; Springer: Berlin, 1986; Vol. 50.

(55) Vauthey, E.; Henseler, A. *J. Phys. Chem.* **1995**, *99*, 8652−8660.

Table 1. Peak Pulse Energy, Beam Waist, and the Maximum Average Intensity for the Incident Beams of the NCP-DFWM Configuration, Assuming $\tau_p = 45$ ps

beam	pulse energy/μJ	beam waist/μm	intensity/(GW cm^{-2})
F-pump	137	150	4.3
B-pump	129	210	2.1
Probe	29	150	0.91

The beam waist is taken as the radial distance at which the intensity fell to $1/e^2$ of its peak value, assuming a cylindrical TEM_{00} mode intensity distribution.

geometry the equivalent association is: Signal, 1, 2, and 3. The maximum energies in the incident beams in the NCP experiment, and their corresponding mean pulse intensities are given in Table 1. Similar pulse energies were used in the FS experiment.

Data Collection and Analysis. The signal pulses are detected by a cooled S1 photomultiplier tube (EMI 9684B), and a computer-controlled neutral-density filter wheel is used to expand the detector dynamic range. Anode pulses are integrated by a charge-sensitive pre-amplifier (Ortec 113A) and fed to one of the inputs of a dual-channel gated integrator, whose digitized output is passed to the computer. The other channel is connected to a photodiode that monitors the attenuated input pulse energy upstream of the beam-splitting optics. To establish the power dependence of the signal, measurements are made as a function of the input intensity, each being the average of a large number of shots. Background determinations are temporally interleaved with these measurements and are made by measuring the signal while blocking the beam which contributes least to the background scattering. In the NCP experiment this is usually the Probe, but for certain tensor components it is more effective to block a beam that is orthogonally polarized to the Signal beam.

The integrated DFWM signal, S_D, usually exhibits a cubic dependence on the integrated incident laser intensity, S_L, as expected for a fast third-order nonlinear optical response. In general, this may involve a number of mechanisms.[50,54,56−65] A fast response occurs when the characteristic relaxation time, τ_r, of the mechanism(s) is short compared to the pulse duration, τ_p.[53,66] In this case, the data can be fitted to $S_D = mS_L^3$, where m is proportional to the product of the square of the path-length, L, and the modulus of the third-order susceptibility, $|\chi^{(3)}|$, and is inversely proportional to the fourth power of the linear refractive index n_0. At each laser intensity setting, the sample and a 100 μm path-length reference cell of CS_2 are introduced alternately into the optical path using a motorized precision translation stage. With these path-lengths the magnitudes of the reference and polymer film signals are similar.

The definition of the third-order susceptibility proposed by Butcher and Cotter is used here.[67] Taking the electric field of a monochromatic optical wave at frequency ω as

$$\vec{E}_m(\vec{r},t) = \frac{1}{2}\{\vec{A}_\omega(\vec{r})\exp[i(\vec{k}_m\cdot\vec{r} - \omega t)] + \text{c.c.}\} \quad (1)$$

where $\vec{A}_\omega$ is the complex amplitude of the field and c.c. denotes the complex conjugate, the Fourier component of the third-order polarization with frequency ω is given by

$$\vec{P}^{(3)}_\omega = \varepsilon_0 \frac{3}{4}\chi^{(3)}(-\omega;\omega,\omega,-\omega)|\vec{A}_\omega\vec{A}_\omega\vec{A}_{-\omega} \quad (2)$$

The sample susceptibility is obtained from the data using[49,52]

$$|\chi^{(3)}|_{\text{Samp}} = |\chi^{(3)}|_{\text{Ref}}\left(\frac{n_{\text{Samp}}}{n_{\text{Ref}}}\right)^2\left(\frac{m_{\text{Samp}}}{m_{\text{Ref}}}\right)^{1/2}\frac{L_{\text{Ref}}}{L_{\text{Samp}}} \quad (3)$$

A value of $n_{\text{Samp}} = 2.0$ at 1064 nm is used for the neat polymer, following Martin's determination made by means of a Kramers−Kronig transformation of the absorption spectrum.[68] The experimental uncertainty in $|\chi^{(3)}|$ is estimated to be ±20% due to the variation in the film thickness. The orientationally averaged third-order molecular polarizability, $\langle\gamma\rangle_{ijkl}$, is related to $\chi^{(3)}_{ijkl}$ by[67]

$$\chi^{(3)}_{ijkl} = N[f(\omega)]^4\langle\gamma\rangle_{ijkl} \quad (4)$$

Here, N is the molecular number density, and $f(\omega)$ is the Lorentz local field factor given by

$$f(\omega) = \frac{[n(\omega)]^2 + 2}{3} \quad (5)$$

In this work, $\tilde{\chi}^{(3)}$ values are reported in SI units, but these may be converted to esu units using

$$\tilde{\chi}^{(3)}[\text{m}^2\,\text{V}^{-2}, \text{SI}] = \left(\frac{4\pi}{9}\times 10^{-8}\right)\tilde{\chi}^{(3)}[\text{cm}^2\,\text{statVolt}^{-2}, \text{esu}] \quad (6)$$

In common with others, we choose for the susceptibility of the CS_2 reference the absolute value obtained by Xuan *et al.* using Jamin interferometry.[69] This choice is justified elsewhere.[50] The actual value used is $\chi^{(3)}_{yyyy} = 3.8\times 10^{-20}$ m^2 V^{-2}, which is obtained by multiplying $\chi^{(3)}_{yyyy}$, as reported by Xuan *et al.*, by a factor of 4 to account for differences between their definition of $\tilde{\chi}^{(3)}$ and that used in this work.

Results

The absorption spectra of neat films and $CHCl_3$ solutions[20] of the porphyrin polymer are similar, with the exception that in the solid films the *Q*-band appears intensified relative to the *B*-band and both bands are slightly blue-shifted relative to their positions in the solution spectrum. Because the *Q*-band is narrow in the solid film, the transparency at the laser wavelength is high ($I/I_0 > 97\%$). The optical quality of the films is good, generating strong DFWM signals with suitably small background scatter. Within the available power range, no signal could be detected above background from the bare substrate.

The power dependence of the DFWM and background signals reveals a sharply defined damage threshold, above which the DFWM signal becomes erratic and the background scatter increases substantially. Figure 4 is a log−log plot of the DFWM signal, $\log(S_D)$, and the background signal, $\log(S_B)$, versus the integrated incident laser intensity, $\log(S_L)$, in the *xyyx* polarization configuration. Straight line fits to the signal and background data below the damage threshold have slopes of 3.17 and 1.06, respectively. A cubic signal power-dependence was found consistently in both the *xyyx* and the *yyyy* configurations. The damage threshold was reproducible at (10 ± 2)% of the maximum laser power, corresponding to a mean intensity of

(56) Zel'dovich, B. Y.; Pilipetsky, N. F.; Shkunov, V. V. *Principles of Phase Conjugation*, Springer Series in Optical Sciences; Springer: Berlin, 1985; Vol. 42.
(57) Gower, M. C. *Prog. Quantum Electron.* **1984**, *9*, 101−147.
(58) Shen, Y. R. *The Principles of Nonlinear Optics*; Wiley: New York, 1984.
(59) Miller, R. J. D.; Casalegno, R.; Nelson, K. A.; Fayer, M. D. *Chem. Phys.* **1982**, *72*, 371.
(60) Fayer, M. D. *Annu. Rev. Phys. Chem.* **1982**, *22*, 63−87.
(61) McEwan, K. J.; Harrison, K. J.; Madden, P. A. *Mol. Phys.* **1990**, *69*, 1025−1042.
(62) Trebino, R.; Barker, C. E.; Siegman, A. E. *IEEE J. Quantum Electron.* **1986**, *22*, 1413−1430.
(63) Lessing, H. E.; von Jena, A. In *Laser Handbook*; Stitch, M. L., Ed.; North-Holland: Amsterdam, 1979; Vol. 3, pp 753−846.
(64) von Jena, A.; Lessing, H. E. *Opt. Quantum Electron.* **1979**, *11*, 419−439.
(65) Maloney, C.; Blau, W. *J. Opt. Soc. Am. B* **1987**, *4*, 1035−1039.
(66) Carter, G. M.; Hryniewicz, J. V.; Thakur, M. K.; Chen, Y. J.; Meyler, S. E. *Appl. Phys. Lett.* **1986**, *49*, 998−1000.
(67) Butcher, P. N.; Cotter, D. *The Elements of Nonlinear Optics*; Cambridge Studies in Modern Optics; Cambridge University Press: Cambridge, 1990; Vol. 9.
(68) Martin, S. J., personal communication, 1995.
(69) Xuan, N. P.; Ferrier, J. L.; Gazengel, J.; Rivoire, G. *Opt. Commun.* **1984**, *51*, 433−437.

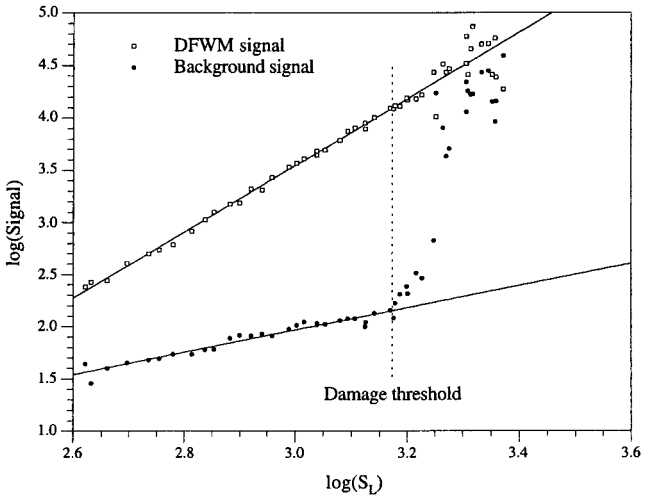

Figure 4. Log−log plot of the DFWM and background signals versus the integrated incident laser intensity for the neat polymer film in the *xyyx* polarization configuration. The smooth curves are fits of a straight line to the data below the damage threshold. The fit to the DFWM signal data has a slope of 3.17 which indicates that the power dependence is cubic. The fit to the background signal has a slope of 1.06, which shows that the background increases linearly with the incident laser power up to the damage threshold.

640 MW/cm^2. The onset of damage is not noticeable to the eye, but pitting can be seen at very high flux (>5 GW/cm^2). The data used for measurements of $|\chi^{(3)}|$ were collected below the damage threshold.

Parts a and b of Figure 5 show the time-resolved NCP-DFWM signal in the *yyyy* configuration when the B-pump and F-pump pulses are delayed. Both consist of a dominant rapid response and a weaker, slowly decaying component. The fwhm of the main features are 50 and 53 ps for delay of the B-pump and F-pump, respectively. Figure 6 shows the data collected in the *xyyx* configuration, together with those obtained for CS_2 when the B-pump is delayed. The dominant contribution to the third-order susceptibility of CS_2 has a relaxation time of ∼2 ps,[70] and thus the trace for CS_2 demonstrates that the signal is pulse-width-limited when the response time is short relative to the pulse duration. The smooth curves in Figure 6 are fits of a Gaussian function to the data. The fwhm of these traces are identical within experimental uncertainty, which shows that the dominant nonlinearity in the polymer film has a response time that is much shorter than 45 ps.

The time-resolved data in the NCP and FS configurations are qualitatively identical. Figure 7 shows the FS signal in the *yyyy* configuration. Delaying either pulse 1 or pulse 2 reveals a dominant pulse-width-limited response accompanied by a very weak long-lived component. When pulse 3 is delayed, no signal can be detected for $\tau_d > 100$ ps because the temporal overlap of pulse 3 with either pulse 1 or 2 is necessary for grating formation. Figure 8 shows the equivalent signals in the *xyyx* configuration. In both cases comparison with the time evolution of the CS_2 signals confirms that the main features are pulse-width limited. In the *xyyx* configuration both NCP and FS data contain no sign of slowly decaying components.

A value of $|\chi^{(3)}_{xyyx}| = (2.9 \pm 0.6) \times 10^{-17}$ m^2 V^{-2} was measured for the polymer film in the NCP experiment, using the signal amplitude at zero delay. The isotropy of the film was

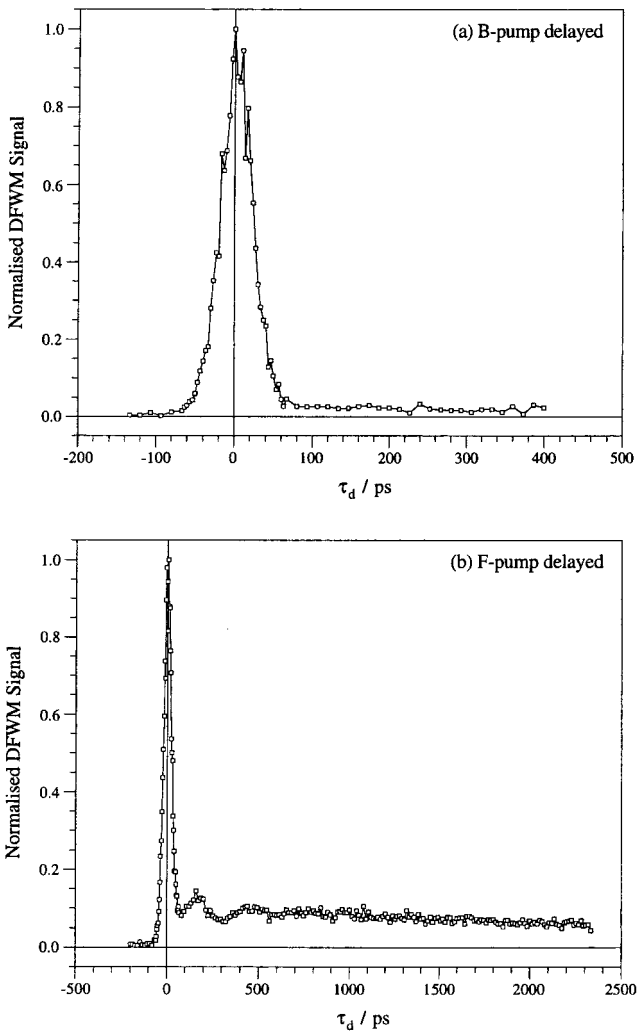

Figure 5. Time-resolved NCP-DFWM signal in the *yyyy* configuration for the polymer film when the (a) B-pump and (b) F-pump are delayed. The fwhm of the sharp features at $\tau_d = 0$ are (a) 50 ps (b) and 53 ps.

confirmed by two separate measurements of $|\chi^{(3)}_{xyyx}|$ in which the film was rotated by 90 degrees between experiments. The values differed by only 5%. $|\chi^{(3)}_{xyyx}|$ was also measured using the FS configuration, and was found to have the value $(2.6 \pm 0.5) \times 10^{-17}$ m^2 V^{-2}, in good agreement with the NCP measurement. The ratio $|\chi^{(3)}_{xyyx}|/|\chi^{(3)}_{yyyy}|$ was 0.27 ± 0.03 and 0.23 ± 0.03 in the NCP and FS configurations, respectively.

A series of measurements was also made on solutions of the polymer, with concentrations in the range 0.1−5.0 mM (per macrocycle) in a 22.5 mM solution of quinuclidine (to reduce aggregation) in $CHCl_3$. These solutions do not obey the Beer−Lambert law at 1064 nm, and it is clear that polymer molecules aggregate. NCP-DWFM measurements of these solutions in a 1 mm cell show a pulse-width-limited response in the *xyyx* configuration, similar to that of the neat thin film. However, the power dependence of the signal was a function of the incident intensity and was only approximately cubic over a limited intensity range. Nonetheless, a rough estimate of the molecular hyperpolarizability $|\langle\gamma\rangle_{xyyx}|$ (per macrocyclic unit) was obtained at a concentration of 5.0 mM (per macrocycle) by comparing the signal with that from the solvent, giving $|\langle\gamma\rangle_{xyyx}| = (1.3 \pm 0.7) \times 10^{-45}$ m^5 V^{-2}.

Discussion

Many of the mechanisms that contribute to third-order optical susceptibilities are not directly related to molecular electronic

(70) Etchepare, J.; Grillon, G.; Astier, R.; Martin, J. L.; Bruneau, C.; Antonetti, A. In *Picosecond Phenomena III*; Eisenthal, K. B., Hochstrasser, R. M., Kaiser, W. Laubereau, A., Eds.; Springer Series in Optical Sciences; Springer: Berlin, 1982; Vol. 23, pp 217−220.

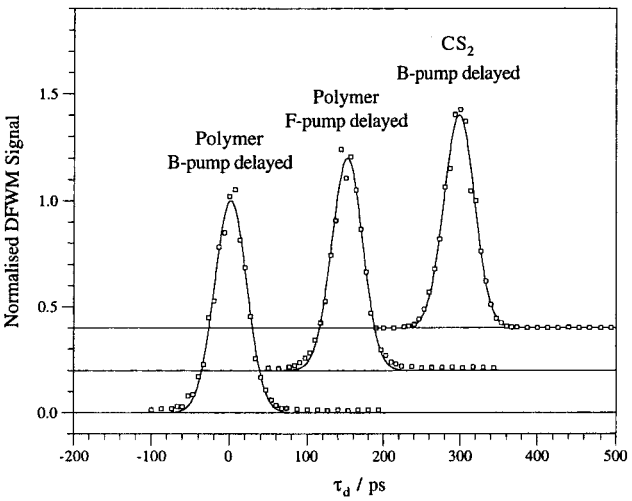

Figure 6. Time-resolved NCP signal in the *xyyx* configuration for the polymer film when the B-pump and F-pump are delayed, and for CS_2 when the B-pump is delayed. The data sets are offset for clarity by intervals of +150 ps on the delay axis and +0.2 on the signal axis. The smooth curves are fits of a Gaussian function to the data. The fwhm are 49 ps (polymer, B-pump delayed), 48 ps (polymer, F-pump delayed), and 46 ps (CS_2).

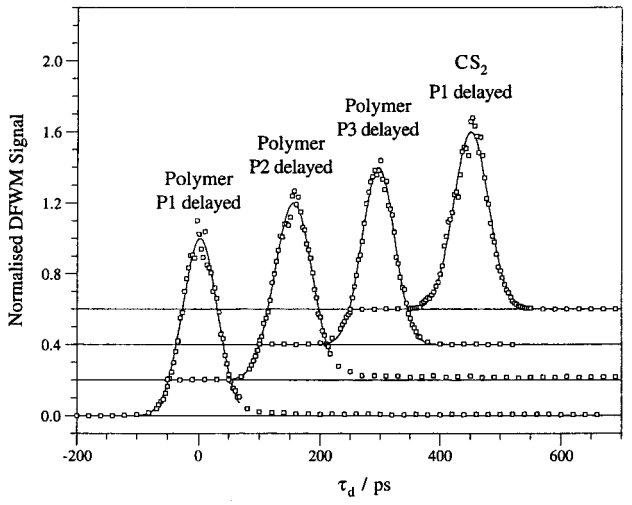

Figure 7. Time-resolved FS signal in the *yyyy* configuration for the polymer film when pulses 1, 2, and 3 are delayed individually and for CS_2 when pulse 1 is delayed. The data sets are offset for clarity by intervals of +150 ps on the delay axis and +0.2 on the signal axis. The smooth curves are fits of a Gaussian function to the data with fwhm of 66 ps (pulse 1 delayed, P1), 73 ps (pulse 2 delayed, P2), and 64 ps (pulse 3 delayed, P3), and 67 ps (CS_2). For the polymer/P1 and polymer/P2 data, the curve fit is restricted to $\tau_d \leq 75$ ps.

properties.[54,56,57,65] We can eliminate several of them on the basis of polarization and time-resolved data, and we will argue that the susceptibility of the porphyrin polymer is dominated by an instantaneous electronic polarizability that is one-photon nonresonant.

First we note from Figures 5−8 that the major component of the nonlinear response occurs within the cross-correlation of the laser pulse, whose fwhm is ∼45 ps. Signals at delays >100 ps occur only in the *yyyy* configuration and are relatively small. This configuration generates spatial intensity modulations, with periods (0.35 and 38 μm) determined by the difference in the wave-vectors of the incident beams.[54] The nature of the material response differs in absorbing and nonabsorbing media.

In absorbing samples the electronic excited-state population density acquires a spatial modulation that is manifest in changes

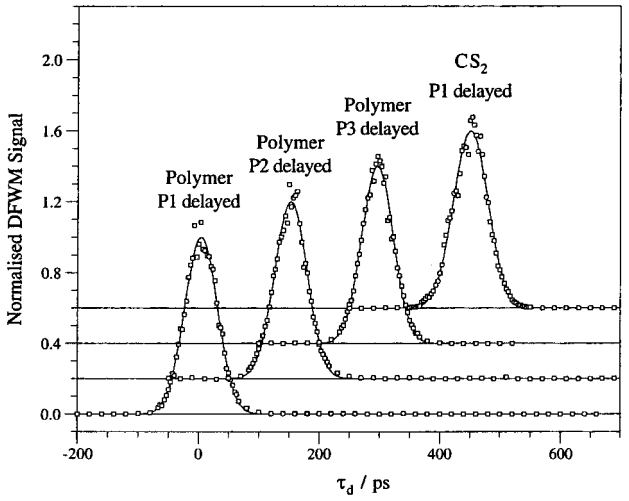

Figure 8. Time-resolved FS-DFWM signal in the *xyyx* configuration for the polymer film when pulses 1, 2, and 3 are delayed individually and for CS_2 in the *yyyy* configuration when pulse 1 is delayed. The data sets are offset by intervals of +150 ps on the delay axis and +0.2 on the signal axis. The smooth curves are fits of a Gaussian function to the data with fwhm of 64 ps (pulse 1 delayed, P1), 63 ps (pulse 2 delayed, P2) and 62 ps (pulse 3 delayed, P3), and 67 ps (CS_2).

to the linear optical polarizability[63,64] and (after a short delay associated with internal energy conversion) to the local temperature and pressure.[60] Diffracted intensity arises from the dependence of the refractive index and absorption coefficient on these perturbations. Following the removal of the optical field, relaxation occurs on a time scale that can be used to identify the mechanism. The change in the optical polarizability can be attributed to the change in electronic structure in the excited state (or states) relative to the ground state, and its relaxation therefore mirrors the electronic ground-state recovery time (typically 10 ps to10 ns). On the other hand, temperature modulations decay on the time scale of thermal diffusion (∼40 ns or 440 μs for the fine and coarse gratings, respectively), while pressure modulations are characterized by the period (∼360 ps and 3.8 μs for the fine and coarse gratings, respectively) of the longitudinal density wave (i.e., acoustic wave) that propagates parallel to the grating vector. Of these only the ground-state recovery time can be short compared to the 45 ps pulse duration.

In nonabsorbing samples spatial index modulations can be generated (a) by nonresonant electronic polarization at the frequency of the driving fields,[54,56,57,61,67] (b) by partial molecular orientation caused by an anisotropy in the induced dipole moments,[54,56,61,62] and (c) by electrostriction, which causes polarizable molecules to redistribute toward the regions of the optical interference pattern where the intensity is maximum (parallel-polarized grating-writing beams only).[54,56,59,61] In the solid porphyrin polymer film molecular orientation can be ruled out, and any electrostrictive displacement would be manifest in an acoustic response that is too slow to account for the observed pulse-width-limited signals.

Polymer **1** is weakly absorbing at 1064 nm, and thus both resonant and nonresonant mechanisms are possible. However, the strong pulse-width limited response occurs on a time scale that is too short to be compatible with any mechanism that involves molecular reorientation or translation, so that the only mechanisms with the correct time scale are those associated with third-order electronic polarization and the population of electronic excited states. This inference is confirmed by time-dependent measurements in the *xyyx* configuration. Here the Probe beam (or beam 3 in the FS geometry) is *x*-polarized, while

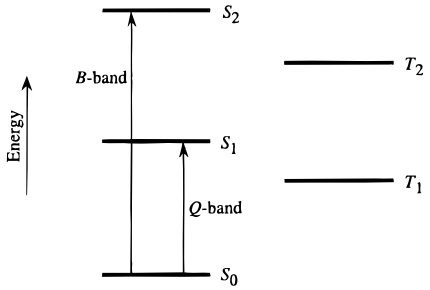

Figure 9. Simplified electronic state diagram for a porphyrin molecule. The *Q*-band is assigned to the $S_0 \rightarrow S_1$ transition and the B-band is assigned to the $S_0 \rightarrow S_2$ transition.

the two beams with which it forms gratings are *y*-polarized. Although the polarization of the resultant optical field is spatially modulated, the intensity remains uniform thereby eliminating the possibility of thermal or acoustic gratings.[54,62] Comparison of Figures 5−8 shows that the weak contributions at long delay times are indeed absent in the *xyyx* configuration. Any refractive index modulation is therefore due to birefringence, whose origin can lie in (a) the third-order electronic polarization and (b) the selective one-photon excitation of molecules whose electronic transition moments contain projections parallel to the optical field.[63,64]

Some understanding of the accessible electronic excited states is needed to identify the nature of the electronic response. O'Keefe *et al.* have examined the transient absorption dynamics of the polymer in solutions of 10% pyridine/$CHCl_3$.[23,24,71] They find that for pump fluences large enough to excite several macrocycles per polymer chain, the ground-state recovery is characterized by a fast and a slow process with time constants of 700 fs and 170 ± 50 ps, respectively. The fast process is assigned to rapid quenching of the excitation via bi-exciton annihilation,[72−74] and the slow process to single exciton decay. The excited states of an individual macrocycle can be described by using the simplified electronic state diagram of Figure 9, which shows the singlet electronic ground state (S_0), and a series of singlet (S_n) and triplet excited states (T_n). Optical excitation creates S_1 excitons, but at high pump fluences, the density of S_1 excitons per polymer chain can be greater than unity, allowing rapid bi-exciton annihilation according to the scheme $S_1 + S_1 \rightarrow S_0 + S_n^*$.[23,73,75] As one excited center returns to the ground state, S_0, a second is promoted to a vibrationally excited higher singlet state S_n^*, which then rapidly relaxes through internal conversion back to S_1. The S_1 population is thus depleted in a period characterized by the fast time constant, until only a single S_1 exciton remains on any given polymer chain. Finally, this relaxes to the ground state in a time characterized by the slow time constant, τ_{S_1}.[23,24] The observed values of τ_{S_1} are typical of singlet lifetimes in non-interacting porphyrins[2,14] and phthalocyanines,[4,75] which vary from hundreds of picoseconds to tens of nanoseconds. Rapid ground-state recovery due to exciton−exciton annihilation is common for porphyrin- and phthalocyanine-based systems in which the excitons are strongly coupled.[8,74,75]

The results of O'Keefe *et al.* are corroborated by independent transient absorption experiments performed by Qureshi and co-workers, who adopt a similar interpretation.[76,77] In their experiments the time constant for the slow process lies in the range 50−300 ps. O'Keefe[71] also found that in a neat polymer film, the slow process is well described by a stretched exponential with a characteristic time of 251 ± 30 ps. Qureshi[77] examined PMMA films loaded to 10 wt % with the polymer and observed that the slow process lengthens to 428 ± 48 ps.

If the DFWM signal for the polymer film in the *xyyx* configuration were due to an excited-state population grating created by optical pumping of S_1, it should decay with time constants comparable to those reported by O'Keefe and Qureshi (251−428 ps) and would be easily observed. The absence of any DFWM signal on this time scale must mean that any contribution from long-lived excited-state gratings is negligible.

The fast response might, however, be a consequence of multiple exciton formation. If the fluence is large enough to excite several macrocycles on a single chain, the response could become pulse-width-limited due to rapid bi-exciton annihilation. Samoc and Prasad have observed this effect in their studies of a film of the perylene dye PTCDA,[78] while Casstevens *et al.* observe a similar shortening of the lifetime of the DFWM signal at high fluences in Langmuir−Blodgett films of phthalocyanines.[9]

Since the time constant for bi-exciton annihilation is much less than τ_p, a multiple exciton grating will decay within the cross-correlation time of the laser pulses, but in doing so it must generate a single exciton grating that persists at large delays. If the susceptibility associated with multiple excitons is significant, the ratio of the pulse-width-limited signal to that remaining at delays corresponding to the single exciton lifetime, when all annihilations are complete, should be a function of the fluence.

It is now possible to distinguish two limiting cases. In the first, the interaction between excitons on the same chain is assumed to be sufficiently weak so that the change in the polarizability is approximately linear in the exciton density. It then follows that the ratio of the signal before and after bi-exciton annihilation should be approximately equal to the square of the number of excitons created per chain[63] and can be estimated as follows. At the damage threshold, the average energy density per pulse is 29 mJ/cm^2, giving a photon density of 1.6×10^{17} photons/cm^2. Assuming that the absorption cross-section at 1064 nm (in the film) is close to that in solution, the cross-section per macrocycle is 1.1×10^{-18} cm^2, and the average number of photons absorbed, per macrocycle, per pulse is 0.18. Thus, for a polymer with 10−15 repeat units, at most 1.8−2.7 photons are absorbed per chain. The ratio of the fast and slow responses should not therefore be greater than 7.3:1. Indeed, this is an upper limit, given that the time-dependent measurements were conducted below the damage threshold. Given that the maximum residual signal in the *xyyx* configuration at $\tau_d \gg \tau_p$ is less than 2% of that at $\tau_d = 0$, this hypothesis is not consistent with the observations.

In the opposite limit it could be assumed that the interaction between excitons on the same chain is strong, leading to a change in the electronic polarizability that is strongly supralinear in exciton density, whereby the magnitude of the fast response component of the signal could become overwhelming. However, this hypothesis implies that the power dependence of the signal amplitude would be strongly hypercubic. Since

(71) O'Keefe, G. E. Ultrafast optical spectroscopy of the excited-states of conjugated organic molecules. Ph.D. Thesis, University of Cambridge, 1996.
(72) Bergman, A.; Levine, M.; Jortner, J. *Phys. Rev. Lett.* **1967**, *18*, 593−596.
(73) Kobayashi, T.; Nagakura, S. *Mol. Phys.* **1972**, *24*, 695−704.
(74) Greene, B. I.; Millard, R. R. *Phys. Rev. Lett.* **1985**, *55*, 1331−1334.
(75) Ho, Z. Z.; Peyghambarian, N. *Chem. Phys. Lett.* **1988**, *148*, 107−111.
(76) Qureshi, F. M.; Thorne, J. R. G.; Bradley, D. D. C.; Anderson, H. L. *Ultrafast relaxations in conjugated porphyrin polymers*; Report: Rutherford-Appelton Laboratory, Central Laser Facility, 1995.
(77) Qureshi, F. M. Nonlinear optical properties of conjugated molecular materials. Ph.D. Thesis, University of Sheffield, UK, 1997.
(78) Samoc, M.; Prasad, P. N. *J. Chem. Phys.* **1989**, *91*, 6643−6649.

Table 2. Measurements of $|\chi^{(3)}|$ by DFWM for Conjugated Polymers[a]

material	$\lvert\chi^{(3)}\rvert$/m^2 V^{-2}	conditions	comments
PMTBQ[b]	2.6×10^{-16}	30 ps CP-DFWM, 532 nm	on-resonance; no time-resolved studies
PPV[c]	3×10^{-17}	400 fs CP-DFWM, 580 and 602 nm	near-resonance; $\tau_r \approx 5$ ps
porphyrin polymer (this work)	$(2.9 \pm 0.6) \times 10^{-17}$	45 ps NCP-DFWM, 1064 nm	off-resonance; *xyyx* element; pulse-width-limited response
polyacetylene[d]	1×10^{-17}	25 ps CP-DFWM, 530 nm	soluble Shirakawa polyacetylene, 20−25 repeat units; on-resonance; pulse-width-limited response
PTS−PDA[e]	7×10^{-18}	300 fs and 6 ps FS-DFWM, 720 nm	off-resonance ($\lambda > 700$ nm); $\tau_r < 300$ fs
PTS−PDA[f]	1.4×10^{-18}	1 ps FS-DFWM, 670−775 nm	near-resonance; $\tau_r \approx 1.6$ ps at 680 nm
PBT[g]	3.0×10^{-19}	1 ps CP-DFWM, 585 and 604 nm	near-resonance; pulse-width-limited response
PPV[h]	3×10^{-19}	1 ps FS-DFWM, 650 nm	near-resonance; pulse-width-limited response reported, although no time-resolved data are presented
4-BCMU−PDA[i]	$(1.8 \pm 0.4) \times 10^{-19}$	33 ps CP-DFWM, 1064 nm	two-photon resonance enhanced; pulse-width-limited response
polypyrrole[j]	1.7×10^{-19}	2 ps CP-DFWM, 584 and 603 nm	on-resonance; $\tau_r \approx 5$ ps
3-BCMU−PDA[i]	$(1.3 \pm 0.3) \times 10^{-19}$	33 ps CP-DFWM, 1064 nm	two-photon resonance enhanced; pulse-width-limited response
PDA[k]	$(1.0 \pm 0.3) \times 10^{-19}$	100 ps CP-DFWM, 532 nm	on-resonance; pulse-width-limited response

[a] The entries are listed in descending values of $|\chi^{(3)}|$. The values have been converted to SI units (in the convention of Butcher and Cotter where possible) and are for the *yyyy* element of $\tilde{\chi}^{(3)}$ unless otherwise stated. Measurements referenced to CS_2 have been recalculated where possible using the absolute value of $\chi^{(3)}_{yyyy}$ adopted in this work. [b] Jenekhe *et al.*[88] PMTBQ is a poly(thiophene) comprised of alternating aromatic and quinoidal repeat units. [c] Singh *et al.*[89] $|\chi^{(3)}|$ was measured for a stretch-oriented film. All incident fields were polarized parallel to the stretch axis. [d] Dorsinville *et al.*[90] $|\chi^{(3)}|$ is referenced to CS_2, but no absolute value is reported. The convention used for $\tilde{\chi}^{(3)}$ is not defined. [e] Carter *et al.*[53,91] $|\chi^{(3)}|$ was measured absolutely. The convention used for $\tilde{\chi}^{(3)}$ is not specified. [f] Schmid *et al.*[85] $|\chi^{(3)}|$ is referenced to CS_2, but no absolute value is reported. The convention of Butcher and Cotter is adopted for $\tilde{\chi}^{(3)}$. [g] Rao *et al.*[92] PBT = poly(*p*-phenylenebenzobisthiazole). $|\chi^{(3)}|$ is referenced to CS_2, but no absolute value is reported. The convention used for $\tilde{\chi}^{(3)}$ is not defined. [h] Bubeck *et al.*[93] $|\chi^{(3)}|$ is referenced to CS_2, but no absolute value is reported. The convention used for $\tilde{\chi}^{(3)}$ is not defined. [i] Nunzi *et al.*[94] The value reported is for the *xyxy* element of the $\tilde{\chi}^{(3)}$ tensor. [j] Ghoshal *et al.*[95] The polypyrrole studied is not fully conjugated due to the occurrence of saturated pyrrole units in the polymer chain. [k] Dennis *et al.*[96] The value reported is for the *xyyx* element of $\tilde{\chi}^{(3)}$.

the experimental power dependence is accurately cubic over a large intensity range (Figure 4), this model can be safely rejected.

To summarize, the rapid response of the observed susceptibility is not compatible either with the known time-dependence of single-exciton excited states, or with plausible multiple exciton densities, or with the anticipated power dependence in the presence of strongly coupled excitons. We are thus led to conclude that the fast-response mechanism cannot be attributed to an excited-state absorption grating and instead must be due to an instantaneous third-order electronic polarization.

The polarization dependence of the *effective susceptibility* can also be used to indicate the relative contributions of various processes (electronic, nuclear, thermal) to the total nonlinearity.[50,54,61,79,80] If the dominant mechanism involves a change in the nuclear coordinates—as is the case for molecular reorientation—theory and experiment show that the tensor ratio $|\chi^{(3)}_{xyyx}|/|\chi^{(3)}_{yyyy}| = 3/4$.[50,61,80] If thermal effects dominate, these will be created in the *yyyy* configuration, but not in the *xyyx* configuration, and thus $|\chi^{(3)}_{xyyx}|/|\chi^{(3)}_{yyyy}| \rightarrow 0$.[54,62] If a third-order electronic polarization dominates, then provided that ω and 2ω are much smaller than the electronic transition frequencies, the Kleinman relations predict that $|\chi^{(3)}_{xyyx}|/|\chi^{(3)}_{yyyy}| = 1/3$.[54,67] Although it is less well-known, it has been shown both theoretically and experimentally that $|\chi^{(3)}_{xyyx}|/|\chi^{(3)}_{yyyy}|$ can also equal 1/3 when the DFWM interaction is dominated by one-photon-resonant excited-state gratings.[13,79,81] Thus, an observation of $|\chi^{(3)}_{xyyx}|/|\chi^{(3)}_{yyyy}| \approx 1/3$ would suggest that an electronic mechanism dominates but is not in itself proof of a resonant or nonresonant mechanism.

For the porphyrin polymer, we find $|\chi^{(3)}_{xyyx}|/|\chi^{(3)}_{yyyy}| = 0.27 \pm 0.03$ (NCP-DFWM) and 0.23 ± 0.03 (FS-DFWM), and thus the most straightforward interpretation of the experimental ratios is that the nonlinearity is electronic. These tensor ratios are smaller than the expected value of 1/3, but this is due in part to contributions from weak long-lived intensity gratings generated in the *yyyy* configuration (Figures 5 and 7). We note also that the assumptions underlying the Kleinman relations are particularly inappropriate in the present system, because of the closeness of the *Q*-band resonance to the optical fundamental. The observation of a tensor ratio that differs significantly from 1/3 is not therefore surprising. Since a one-photon resonant electronic nonlinearity is ruled out by the fast time-response, we conclude that the susceptibility ratio indicates the dominance of a one-photon nonresonant electronic polarization.

Since the signal detected in the *xyyx* configuration must arise from a pure one-photon nonresonant electronic effect, we focus on the susceptibility measured in this configuration. After accounting for local field factors in the solid film, the third-order polarizability per macrocycle is found to be $|\langle\gamma\rangle_{xyyx}| = (4.1 \pm 1.2) \times 10^{-45}$ m^5 V^{-2}. This compares well with the solution estimate of $|\langle\gamma\rangle_{xyyx}| = (1.3 \pm 0.7) \times 10^{-45}$ m^5 V^{-2}, given the uncertainty in the latter value. Elsewhere we have shown that solution measurements for the monomer of **1** yield $|\langle\gamma\rangle_{xyyx}| = (4.8 \pm 2.4) \times 10^{-48}$ m^5 V^{-2}.[50] Clearly, the effective unit susceptibility of the polymer is dramatically enhanced relative to that of the monomer; indeed, its large magnitude must be attributed to extensive electronic delocalization in the conjugated π-system.[82,83]

Comparison with Related Materials

The measured value of $|\chi^{(3)}|$ for the porphyrin polymer can be compared with those of other highly conjugated polymers, particularly those of polyacetylene and polydiacetylene, which are recognized as being among the materials possessing the largest fast-response nonlinearities currently available.[82,84,85] Table 2 lists values of $|\chi^{(3)}|$ which have been measured by

(79) Deeg, F. W.; Fayer, M. D. *J. Chem. Phys.* **1989**, *91*, 2269−2279.
(80) Bourdin, J. P.; Nguyen, P. X.; Rivoire, G.; Nunzi, J. M. *Mol. Cryst. Liq. Cryst. Sci. Technol., Sec. B Nonlinear Opt.* **1994**, *7*, 1−6.
(81) Myers, A. B.; Hochstrasser, R. M. *IEEE J. Quantum Electron.* **1986**, *22*, 1482.
(82) Kajzar, F.; Messier, J. In *Conjugated Polymers: The Novel Science and Technology of Highly Conducting and Nonlinear Optically Active Materials*; Brédas, J.-L., Silbey, R., Eds.; Kluwer Academic Publishers: Dordrecht, 1991; pp 509−554.
(83) Nalwa, H. S. In *Nonlinear Optics of Organic Molecules and Polymers*; Nalwa, H. S., Miyata, S., Eds.; CRC Press: New York, 1997; pp 611−797.
(84) Etemad, S.; Baker, G. L. *Synth. Met.* **1989**, *28*, D159−D166.
(85) Schmid, W.; Vogtmann, T.; Schwoerer, M. *Chem. Phys.* **1996**, *204*, 147−155.

DFWM for several conjugated polymers at a variety of wavelengths, and it is immediately obvious that polymer **1** is one of the most nonlinear materials. In making comparisons it should also be borne in mind that the value of $|\chi^{(3)}|$ listed for the porphyrin polymer is for the *xyyx* element, whereas most of the other measurements are of the *yyyy* element, which by the arguments of Kleinman symmetry will be of the order of 3 times larger. The large value of $|\chi^{(3)}|$ for the porphyrin polymer is corroborated by the quadratic electroabsorption studies of Martin and co-workers.[18,20]

The Stegeman figures-of-merit W and T are measures of the maximum optically induced phase shift that is possible within the characteristic absorption length due to linear and two-photon processes, respectively.[1,86] Useful devices become possible if $W > 1$ and $T < 1$. To obtain these parameters for the porphyrin polymer we assume that $\tilde{\chi}^{(3)}$ is entirely real and positive and that Kleinman symmetry holds, and calculate an intensity dependent refractive index $n_2^{(I)} = 6.2 \times 10^{-15}$ m^2 W^{-1}.[67] Using the average intensity at the damage threshold (640 MW/cm^2) yields the value $W = 0.7$. *Z*-scan measurements at 1064 nm by Qureshi[77] yield the two-photon intensity absorption coefficient $\alpha_2^{(I)} = 9.3 \times 10^{-10}$ m W^{-1}, from which we calculate $T = 0.32$.

Although the porphyrin polymer falls short of the transparency requirement that $W > 1$ at 1064 nm, W is expected to increase with wavelength, since the residual linear absorption falls sharply beyond 900 nm. Thus, measurements at wavelengths within the telecommunications window would be particularly valuable. The potential for a material with a nonlinearity of this magnitude is indicated by the observation that, at the damage threshold, a Mach−Zender based switch would require a path length of only 50 μm. However, practical devices would have to operate at much lower average powers, given the thermal dissipation implied by the residual linear absorption and its consequences for the stability of the optical constants of a waveguide interferometer.

Most other conjugated polymers have been studied at wavelengths at which they absorb strongly (see Table 2). For these, the DFWM interaction is predominantly one-photon resonant, and in many cases (e.g., PPV, PTS−PDA, and polypyrrole) the time-resolved responses are not pulse-width-limited. Although some of the on-resonance measurements listed in Table 2 do appear to be pulse-width-limited, this is presumably because the pulse duration was significantly longer than the ground-state recovery time.[53]

The only materials in Table 2 which outperform polymer **1** in terms of the magnitude of the susceptibility (PMTBQ and PPV) have been examined on- or near resonance, where the response is inevitably noninstantaneous. If these are ignored, on the grounds that they are either too absorbing or too slow for device applications, and the Kleinman relations are used as a guide to the ratio of the elements of $\tilde{\chi}^{(3)}$, then polymer **1** has a susceptibility that is more that 10 times larger than the nearest comparable material, i.e., PTS−PDA. Resonant enhancement can increase the susceptibility by several orders of magnitude,[58,67] and thus those materials for which data were obtained on-resonance are unlikely to have off-resonance susceptibilities as large as that of the porphyrin polymer.

Conclusion

The third-order nonlinear optical properties of a novel conjugated porphyrin polymer have been studied using degenerate four-wave mixing at 1064 nm. Two elements of the third-order susceptibility tensor have been measured. Time-resolved experiments indicate that the nonlinear optical response is very rapid (response time $\ll$ 45 ps) and one-photon nonresonant. An analysis of these results, together with data obtained by others, shows that the nonlinearity originates from a true third-order electronic polarization. Relative to the monomer, the microscopic polarizability per macrocycle of the polymer is higher by 3 orders of magnitude, showing that the large nonlinearity results from the extensive electronic delocalization in the conjugated π-system. A comparison of polymer **1** with other systems reveals that it possesses one of the largest nonlinearities of any conjugated organic polymer studied to date, and the largest among those studied off-resonance by over a factor of 10. This finding is particularly striking because alternative polymers are only competitive on-resonance, in which case losses and slow response times render them unsuitable for real applications. We note that in addition to its very large optical nonlinearity, polymer **1** is representative of a novel class of robust, highly processible, and easily derivatized conjugated polymers. Efforts are being undertaken to further characterize the optical nonlinearity of this material[87] and to identify ways of enhancing the optical properties through further structural modifications.

Acknowledgment. This material is based upon work supported by a National Science Foundation Graduate Research Fellowship (to S.M.K.) and by the Engineering and Physical Sciences Research Council. S.M.K. gratefully acknowledges support from the Marshall Aid Commemoration Commission and St. Catherine's College, Oxford, UK. We thank Pedrode Oliveira for performing the AFM measurements.

JA9922330

(86) Stegeman, G. I. In *Contemporary Nonlinear Optics*; Agrawal, G. P., Boyd, R. W., Eds.; Academic: Boston, 1992; pp 1−40.

(87) Thorne, J. R. G.; Kuebler, S. M.; Denning, R. G.; Blake, I. M.; Taylor, P. N.; Anderson, H. L. *Chem. Phys.* **1999**, *248*, 181−193.

(88) Jenekhe, S. A. *Appl. Phys. Lett.* **1989**, *54*, 2524−2526.

(89) Singh, B. P.; Prasad, P. N.; Karasz, F. E. *Polymer* **1988**, *29*, 1940−1942.

(90) Dorsinville, R.; Yang, L.; Alfano, R. R.; Tubino, R.; Destri, S. *Solid State Commun.* **1988**, *68*, 875−877.

(91) Carter, G. M.; Thakur, M. K.; Chen, Y. J.; Hryniewicz, J. V. *Appl. Phys. Lett.* **1985**, *47*, 457−459.

(92) Rao, D. N.; Swiatkiewicz, J.; Chopra, P.; Ghoshal, S. K.; Prasad, P. N. *Appl. Phys. Lett.* **1986**, *48*, 1187−1189.

(93) Bubeck, C.; Kaltbeitzel, A.; Neher, D.; Stenger-Smith, J. D.; Wegner, G.; Wolf, A. In *Electronic Properties of Conjugated Polymers III*; Kuzmany, H., Mehring, M., Roth, S., Eds.; Springer Series in Solid-State Sciences; Springer: Berlin, 1989; Vol. 91, pp 214−219.

(94) Nunzi, J. M.; Grec, D. *J. Appl. Phys.* **1987**, *62*, 2198−2202.

(95) Ghoshal, S. K. *Chem. Phys. Lett.* **1989**, *158*, 65−69.

(96) Dennis, W. M.; Blau, W.; Bradley, D. J. *Appl. Phys. Lett.* **1985**, *47*, 200−202.